DALTON
FULL PAPER

Selectivity of sterically efficient $[HB(pz)_3]^-$ and crowded $[B(pz)_4]^-$ for first-series transition metals and Cd †

Tsuyoshi Kitano,*[a] Yoshiki Sohrin,[a] Yasuo Hata,[a] Hitoshi Kawakami,[b] Takeyoshi Hori[b] and Kazumasa Ueda[b]

[a] *Institute for Chemical Research, Kyoto University, Uji, Kyoto 611-0011, Japan*
[b] *Faculty of Technology, Kanazawa University, 2-40-20 Kodatsuno, Kanazawa 920-8667, Japan*

Received 6th July 2001, Accepted 17th October 2001
First published as an Advance Article on the web 20th November 2001

Separation of first-series transition metal ions {Mn(II), Fe(II), Co(II), Ni(II), Cu(II) and Zn(II)} and Cd(II) has been studied by solvent extraction using $[HB(pz)_3]^-$ and $[B(pz)_4]^-$. These ligands quantitatively extract all the studied metal ions. $[HB(pz)_3]^-$ is one of the most powerful extractants of these metal ions, since it extracts them from acidic aqueous solution (pH 2.1). $[B(pz)_4]^-$ extracts large metal ions, such as Mn(II) and Cd(II), around higher pH compared to $[HB(pz)_3]^-$. Also, the extraction constant of $[B(pz)_4]^-$ for Cu(II) is low and does not conform to the order of the Irving–Williams series. The different selectivity of these ligands cannot be explained on the basis of the basicity of the donor atoms. To explore the origin of the selectivity, X-ray crystal structures of the six extracted species have been determined. The complexes of $[HB(pz)_3]_2Mn$ (**1**), $[B(pz)_4]_2Mn$ (**2**), $[B(pz)_4]_2Co$ (**3**), $[B(pz)_4]_2Ni$ (**4**), and $[B(pz)_4]_2Zn$ (**6**) have distorted octahedral geometries with each ligand having tridentate coordination. The complex $[B(pz)_4]_2Cu$ (**5**) has square bipyramidal geometries. Examination of the dimensions of the above-mentioned complexes and the eight related ones has revealed that although the $[HB(pz)_3]^-$ complexes are highly C_3 symmetric, the $[B(pz)_4]^-$ complexes for Mn(II), Cu(II) and Cd(II) are largely distorted. These results suggest that $[HB(pz)_3]^-$ is sterically efficient, and the increase in steric energy with complex formation is sufficiently low. On the other hand, because of the intraligand contact between pyrazolyl rings, $[B(pz)_4]^-$ accompanies substantial steric energy increases in coordination to Mn(II), Cu(II) and Cd(II), decreasing the stability of the complexes and resulting in unique selectivity.

Introduction

Recent studies on complex formation have revealed that the ligand structure plays a critical role in selectivity for metal ions.[1] The stability of complexes with conventional chelating ligands is governed by the chelate ring size. For example, the increase in chelate ring size from five-membered, formed by ethylenediaminetetraacetic acid, to six-membered, formed by trimethylenediaminetetraacetic acid, leads to a sharp decrease in formation constant to the large metal ions. Trifluoroacetylcyclopentanone is a stronger extractant for lanthanoid ions than trifluoroacetylcyclohexanone.[2] The stability of complexes with macrocyclic ligands is governed by the cavity size.[3] It is especially obvious in rigid and preorganized macrocycles that the most stable complex is formed when the cation diameter matches the cavity size.

In previous reports,[4] we have shown that poly(pyrazolyl)borates, of which the basic structure is $[H_nB(pz)_{4-n}]^-$ (n = 0–2), have a unique selectivity for metal ions due to different steric factors from the conventional ligands. The selectivity of tripodal tridentate ligands, $[HB(pz)_3]^-$ and $[B(pz)_4]^-$, for Group 2 metal ions was studied by solvent extraction.[4c] $[HB(pz)_3]^-$ formed octahedral A_2M complexes with Mg^{2+}, Ca^{2+} and Sr^{2+}, and extracted Mg^{2+} and Ca^{2+} effectively and Sr^{2+} to some extent. However, $[B(pz)_4]^-$ extracted Mg^{2+} but not Ca^{2+}, because it is hard for $[B(pz)_4]^-$ to increase the bite size due to intraligand contact between pyrazolyl rings and $[B(pz)_4]_2Ca$ was not stable enough to be extracted.

Here we report the results of solvent extraction of Mn(II), Fe(II), Co(II), Ni(II), Cu(II), Zn(II) and Cd(II) with $[HB(pz)_3]^-$ and $[B(pz)_4]^-$. $[HB(pz)_3]^-$ was found to be the more powerful extractant for these metal ions. The extractability for metal ions, such as Mn(II), Cu(II) and Cd(II), was substantially decreased with $[B(pz)_4]^-$. To explore the origin of the selectivity X-ray crystal structures of the extracted species, such as $[HB(pz)_3]_2Mn$ (**1**), $[B(pz)_4]_2Mn$ (**2**), $[B(pz)_4]_2Co$ (**3**), $[B(pz)_4]_2Ni$ (**4**), $[B(pz)_4]_2Cu$ (**5**) and $[B(pz)_4]_2Zn$ (**6**), have been determined. The X-ray structures of the 14 complexes of $[HB(pz)_3]^-$ and $[B(pz)_4]^-$ with Mn(II), Fe(II), Co(II), Ni(II), Cu(II), Zn(II) and Cd(II) are compared precisely and steric factors controlling the selectivity are discussed.

Results

Acid dissociation and partition constants of ligands

Poly(pyrazolyl)borates are polyprotic bases. The acid dissociation constants are defined as:

$$K_{a1} = [H^+][HA]/[H_2A^+] \quad (1)$$

$$K_{a2} = [H^+][A^-]/[HA] \quad (2)$$

where square brackets represent the molar concentration in aqueous solution and A^- stands for the poly(pyrazolyl)borate anion. The partition constant of the ligand is defined as:

$$P_{HA} = [HA]_o/[HA] \quad (3)$$

where the subscript o denotes the species in the organic phase. The logarithm of the distribution ratio of the ligand (log D_{HA})

† Electronic supplementary information (ESI) available: experimental details. See http://www.rsc.org/suppdata/dt/b1/b106006f/

 DOI: 10.1039/b106006f

between the aqueous and chloroform phases was plotted as a function of pH:

$$D_{HA} = [HA]_o/([H_2A^+] + [HA] + [A^-]) = P_{HA}/([H^+]/K_{a1} + 1 + K_{a2}/[H^+]) \quad (4)$$

The plot was analyzed by a non-linear least-squares method and the partition and acid dissociation constants were obtained. The poly(pyrazolyl)borates were hydrolyzed in water into pyrazole and boric acid. In the distribution experiment, the ligand concentrations in the organic phase decreased with an increase in shaking time (t min). The decomposition rate was highest around pH 3–8 for $[HB(pz)_3]^-$ and 2–7 for $[B(pz)_4]^-$. To remove the influence of hydrolysis, log $[HA]_o$ was plotted against t. The value at $t = 0$ was obtained by extrapolation and used for plots of log D_{HA} *vs.* pH. For hydrotris(pyrazolyl)-borate, pK_{a1}, pK_{a2} and log P_{HA} were 3.40, 7.37 and 0.23, respectively. For tetrakis(pyrazolyl)borate, pK_{a1}, pK_{a2} and log P_{HA} were 2.58, 6.08 and 0.98, respectively. The acid dissociation constants mostly agreed with those obtained by the titration method.

Extraction of transition metals

The %E of the metal ions reached a maximum within 60 min of shaking and decreased when the shaking time was prolonged, especially for Cd(II) because of decomposition of the ligand at this pH. Thus, 60 min of shaking was adopted for the following experiments. The %E is plotted as a function of pH in Fig. 1.

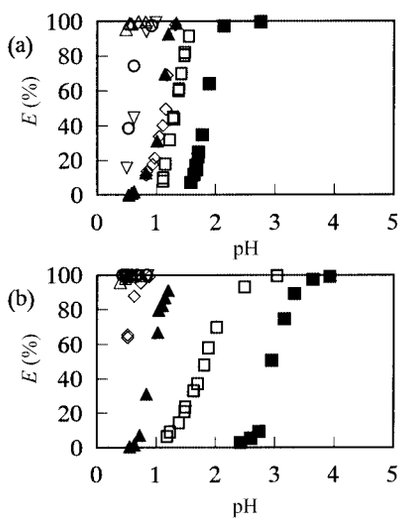

Fig. 1 Effect of pH on the percentage extraction of metal ions. Aqueous phase: 1×10^{-2} M KA, 1×10^{-2} M buffer, 1×10^{-4} M M^{2+} (10 mL). Organic phase: chloroform (10 mL). Key: (a) K[HB(pz)$_3$]; (b) K[B(pz)$_4$]. ■ Mn(II); ◇ Fe(II); ▽ Co(II); ○ Ni(II); △ Cu(II); ▲ Zn(II); □ Cd(II).

The %E was independent of the metal ion concentration of 3×10^{-5}–3×10^{-4} M. All the studied metal ions were quantitatively extracted into the chloroform phase. It should be especially noted that $[HB(pz)_3]^-$ is able to quantitatively extract Cd(II) and Mn(II) at a low pH of 2.1. $[HB(pz)_3]^-$ is one of the most powerful extractants to these metal ions as far as we know. With $[B(pz)_4]^-$, Fe(II), Co(II), Ni(II) and Cu(II) are extracted at lower pH compared with $[HB(pz)_3]^-$, while Mn(II) and Cd(II) are extracted at higher pH.

In order to obtain the extraction constants for the metal ions, the logarithm of distribution ratio for the metal ion (log D) was measured using the aqueous phase containing [HCl] + [LiCl] = 1.5 M:

$$D = C_{M,o}/C_M \quad (5)$$

Table 1 Extraction constants (log K_{ex}) of first-series transition metals with $[H_2B(pz)_2]^-$, $[HB(pz)_3]^-$, and $[B(pz)_4]^-$

	$[H_2B(pz)_2]^-$ [a]	$[HB(pz)_3]^-$	$[B(pz)_4]^-$
Mn(II)	−7.56	3.3	0.5
Fe(II)	−4.36	4.8	3.5
Co(II)	−1.49	6.3	6.0
Ni(II)	−0.86	9.2	8.8
Cu(II)	5.81	9.6	6.9
Zn(II)	0.75	6.2	3.7
Cd(II)		4.4	1.2

[a] Data taken from ref. 4*f*. Aqueous phase: 1×10^{-2} M KA or HA, 2×10^{-2} M buffer, 0.1 M potassium chloride, 1×10^{-4} M M^{2+} (10 mL).

where C_M signifies the analytical molar concentration of the metal ion (M^{2+}). The overall extraction equilibrium and extraction constant (K_{ex}) of the metal ion can be described as:

$$M^{2+} + 2HA_o \rightleftarrows A_2M_o + 2H^+ \quad (6)$$

$$K_{ex} = [A_2M]_o[H^+]^2/[M^{2+}][HA]_o^2 \quad (7)$$

$$\log K_{ex} = \log D + 2 \log [H^+] - 2 \log [HA]_o \quad (8)$$

To analyze the extraction data graphically, the protonation and distribution of the ligands must be taken into consideration. $[HA]_o$ is expressed as:

$$[HA]_o = C_{HA}/\alpha \quad (9)$$

$$\alpha = 1 + \{[H^+]/K_{a1} + 1 + K_{a2}/[H^+]\}/P_{HA} \quad (10)$$

where C_{HA} means the initial concentration of the ligand in the aqueous phase. Substitution of eqn. (9) into (8) and rearrangement results in:

$$\log D - 2 \log C_{HA} + 2 \log \alpha = -2 \log [H^+] + \log K_{ex} \quad (11)$$

We investigated the dependence of log D − 2 log C_{HA} + 2 log α on −log $[H^+]$ for all the ligands and metals. All of the plots gave straight lines with slopes close to 2. These results imply that the change in activity coefficient of H^+ is negligible under the experimental conditions and confirm the validity of eqn. (6). The log K_{ex} values, which were obtained from the plots by a linear least-squares fit, are listed in Table 1 in comparison with those for $[H_2B(pz)_2]^-$. Since the definition of eqn. (6) has been altered from that in our previous report,[4f] the log K_{ex} values have been recalculated for $[H_2B(pz)_2]^-$.

Synthesis of complexes

Complexes with two poly(pyrazolyl)borate ligands coordinated to the bivalent metal ions were produced according to the equation:

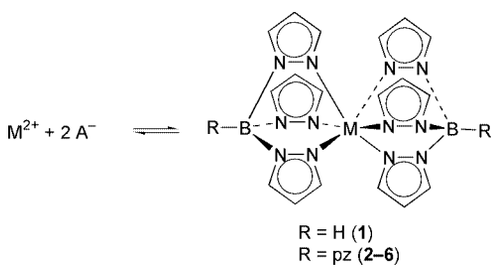

(12)

R = H (**1**)
R = pz (**2–6**)

These complexes were obtained as precipitates and dissolved in dichloromethane, chloroform, and diethyl ether. All of them were stable in air.

Structure of the complexes

There are two crystallographically independent molecules within a unit cell of complexes **1**, **3**, **4**, **5**, and **6**. For these complexes the distances between the metal ion and the donor atom are slightly but systematically different. The manganese atom of complex **2** is located on an inversion center of a unit cell. In complex **1**, the two manganese atoms are lying on different inversion points in the crystal. Fig. 2, 3, and 4 show

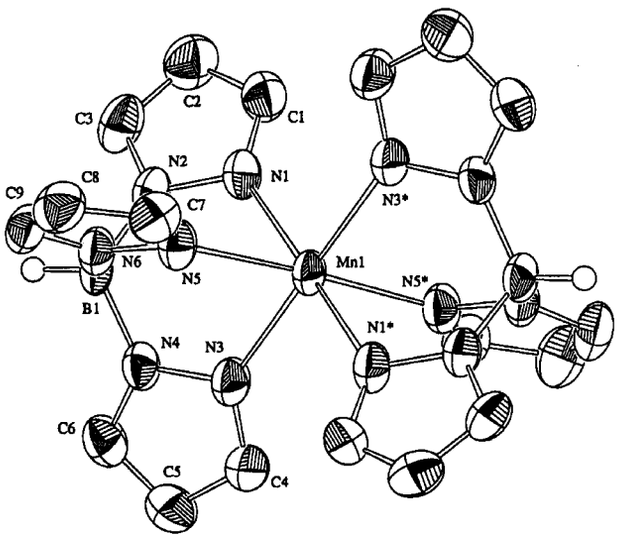

Fig. 2 ORTEP view of $[HB(pz)_3]_2Mn$ (**1**) (50% probability). Hydrogen atoms are omitted for clarity except the hydrogen atoms bonded to boron atoms.

ORTEP drawings of a molecule of **1**, **2**, and **5**, respectively. The molecules of **3**, **4**, and **6** are similar to that of **2**. Tables 2–7 show selected bond distances and angles of **1**–**6**, respectively. The molecule is monomeric with no short intermolecular contacts. Both ligands are tridentate and the geometry about the metal atom is a trigonally distorted octahedron except **5** which is a square bipyramid. In complex **5**, the bond distances between the copper atom and the coordinated nitrogen atoms of each ligand differ significantly. The longest bond distance is 0.41 Å longer than the remainder. In complexes **2**–**6**, the nonco-ordinated pyrazolyl rings stand out in the direction opposite the metal atom.

The mean dimensions of chelate rings for the studied and related complexes[5] are summarized in Table 8; the labeling of atoms is given in Scheme 1.

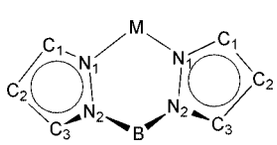

Scheme 1

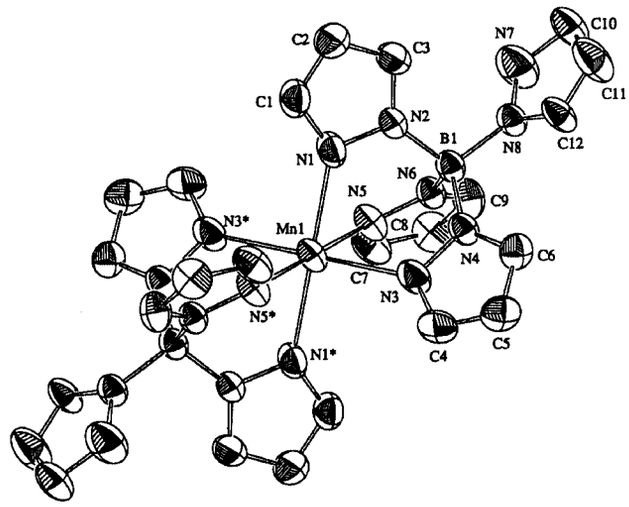

Fig. 3 ORTEP view of $[B(pz)_4]_2Mn$ (**2**) (50% probability). Hydrogen atoms are omitted for clarity.

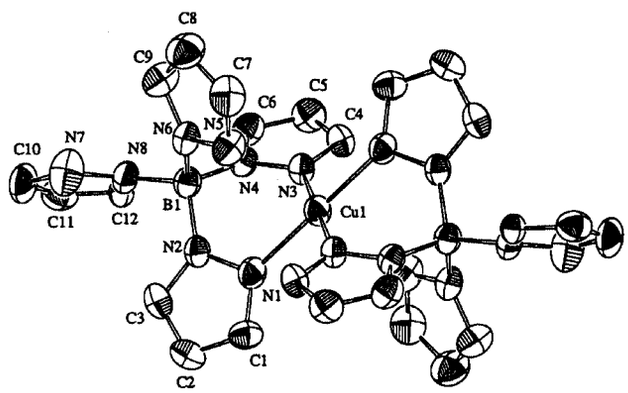

Fig. 4 ORTEP view of $[B(pz)_4]_2Cu$ (**5**) (50% probability). Hydrogen atoms are omitted for clarity.

Discussion

Extractability of $[H_2B(pz)_2]^-$, $[HB(pz)_3]^-$ and $[B(pz)_4]^-$

The three polypyrazolylborates quantitatively extract Mn(II), Fe(II), Co(II), Ni(II), Cu(II), Zn(II) and Cd(II) into chloroform. The extracted species with these ligands are A_2M. However, the K_{ex} values are very different among the ligands (Table 1). $[HB(pz)_3]^-$ shows the highest K_{ex} for all the metal ions. The trend of K_{ex} for $[HB(pz)_3]^-$ and $[H_2B(pz)_2]^-$ was in accordance with the common Irving–Williams series in stability constants. The K_{ex} values for Co(II) and Ni(II) with $[B(pz)_4]^-$ are similar to those with $[HB(pz)_3]^-$. However, the K_{ex} values for Mn(II), Cu(II), Zn(II) and Cd(II) with $[B(pz)_4]^-$ are substantially lower than those with $[HB(pz)_3]^-$.

Table 2 Selected bond distances (Å) and bond angles (deg) for $[HB(pz)_3]_2Mn$ (**1**)

	Molecule 1		Molecule 2
Mn(1)–N(1)	2.263(5)	Mn(2)–N(7)	2.223(4)
Mn(1)–N(3)	2.197(4)	Mn(2)–N(9)	2.285(5)
Mn(1)–N(5)	2.265(5)	Mn(2)N(11)	2.272(5)
N(1)–Mn(1)–N(1*)	101.8(2)	N(7)–Mn(2)–N(7*)	179.4(3)
N(1)–Mn(1)–N(3)	84.7(2)	N(7)–Mn(2)–N(9)	84.8(2)
N(1)–Mn(1)–N(5)	81.0(2)	N(7)–Mn(2)–N(11)	84.3(2)
N(3)–Mn(1)–N(3*)	177.3(3)	N(9)–Mn(2)–N(9*)	99.2(3)
N(3)–Mn(1)–N(5)	85.3(2)	N(9)–Mn(2)–N(11)	80.2(2)
N(5)–Mn(1)–N(5*)	96.1(2)	N(11)–Mn(2)–N(11*)	100.4(2)
Mn(1)–N(1)–N(2)	116.5(3)	Mn(2)–N(7)–N(8)	118.9(3)
Mn(1)–N(3)–N(4)	120.0(3)	Mn(2)–N(9)–N(10)	117.0(4)
Mn(1)–N(5)–N(6)	117.5(4)	Mn(2)–N(11)–N(12)	117.2(3)

The K_{ex} is represented as:

$$K_{ex} = P_{A2M}\beta_{A2M}K_{a2}^2/P_{HA}^2 \quad (13)$$

where P_{A2M} is the partition constant and β_{A2M} is the stability constant for the A_2M complex. The values of P_{HA} for $[H_2B(pz)_2]^-$, $[HB(pz)_3]^-$ and $[B(pz)_4]^-$ are 1.58,[4b] 1.60 and 9.77, respectively. Although we do not know the P_{A2M} values, it seems that the above-mentioned features of K_{ex} are not dominated by P_{A2M}/P_{HA}^2. The fact that $[HB(pz)_3]^-$ and $[B(pz)_4]^-$ have higher extractability for all the studied metal ions than $[H_2B(pz)_2]^-$ may be attributed to the following two aspects. The first point is the values of pK_{a2}. The values of pK_{a2} for $[H_2B(pz)_2]^-$, $[HB(pz)_3]^-$ and $[B(pz)_4]^-$ are 8.72,[4b] 7.35 and 6.08, respectively. These values are higher than that of pyrazole ($pK_a = 2.60$).[6] The basicity of the coordinating nitrogen atoms of the ligands is increased in comparison with that in the pyrazole molecule because of electron donation from the central boron atom to the pyrazolyl groups. When the number of pyrazolyl groups is increased, the electron donation per pyrazolyl group is decreased, so the value of pK_{a2} is decreased. The second point is the increase of β_{A2M}. Although $[H_2B(pz)_2]^-$ acts as a bidentate ligand and forms a tetrahedral or square planar complex, $[HB(pz)_3]^-$ and $[B(pz)_4]^-$ act as tridentate ligands and form octahedral complexes. It is thought that the stability constants of the complexes with $[HB(pz)_3]^-$ and $[B(pz)_4]^-$ are enhanced due to the additional chelate effect. However, the difference in K_{ex} between $[HB(pz)_3]^-$ and $[B(pz)_4]^-$ cannot be explained on the basis of electronic effects and conventional chelate effects. It is apparently strange that $[HB(pz)_3]^-$ is a stronger extractant than $[B(pz)_4]^-$ although the lower pK_{a2} of $[B(pz)_4]^-$ is more favorable for extraction. It is very likely that the tendency of K_{ex} is mainly controlled by the change in β_{A2M} caused by steric effects. Examination of the structure of the extracted species is essential in order to elucidate the above-mentioned problems. Thus, the extracted species were synthesized and their structures were determined by X-ray crystallography.

Table 3 Selected bond distances (Å) and bond angles (deg) for $[B(pz)_4]_2Mn$ (**2**)

Mn(1)–N(1)	2.201(3)	N(1)–Mn(1)–N(1*)	180.0
Mn(1)–N(3)	2.223(3)	N(1)–Mn(1)–N(3)	85.9(1)
Mn(1)–N(5)	2.283(3)	N(1)–Mn(1)–N(5)	81.5(1)
		N(3)–Mn(1)–N(3*)	180.0
		N(3)–Mn(1)–N(5)	80.7(1)
		N(5)–Mn(1)–N(5*)	180.0
		Mn(1)–N(1)–N(2)	118.7(2)
		Mn(1)–N(3)–N(4)	121.8(2)
		Mn(1)–N(5)–N(6)	117.2(2)

Sterically efficient structure of $[HB(pz)_3]^-$

In all the studied and related $[HB(pz)_3]^-$ complexes, the pyrazolyl rings are planar, in which carbon and hydrogen atoms are oriented radially away from the B ··· M ··· B axis. This structure is quite favorable for trigonal tridentate coordination. $[HB(pz)_3]^-$ can adopt a conformation suitable for tridentate coordination without severe intraligand contact. On the basis of molecular mechanics calculations, the increase in strain energy[4d] is only some 1.0 kcal mol^{-1} when the free ligand is taken from the lowest strain energy configuration and coordinated to a metal ion. Further, the mutually staggered conformation prevents the interligand contact, favoring formation of the six-coordinate A_2M complex. Fig. 5 (left) shows a ball and stick model of $[HB(pz)_3]_2Fe$ (**7**) viewed from the C_3 axis (B ··· M ··· B). The increase in steric hindrance accompanying the A_2M complex formation should be fairly small. That is, $[HB(pz)_3]^-$ is sterically efficient at occupying a six-coordination. This is the structural reason why $[HB(pz)_3]^-$ is the most powerful extractant.

Table 8 shows that the average M–N1 distances are nearly equal to the sum of Shannon's ionic radii.[7] The radii of the

Table 4 Selected bond distances (Å) and bond angles (deg) for $[B(pz)_4]_2Co$ (**3**)

	Molecule 1		Molecule 2
Co(1)–N(1)	2.164(4)	Co(2)–N(9)	2.135(4)
Co(1)–N(3)	2.074(4)	Co(2)–N(11)	2.106(4)
Co(1)–N(5)	2.126(4)	Co(2)–N(13)	2.127(4)
N(1)–Co(1)–N(1*)	180.0	N(9)–Co(2)–N(9*)	180.0
N(1)–Co(1)–N(3)	85.2(1)	N(9)–Co(2)–N(11)	86.7(1)
N(1)–Co(1)–N(5)	83.6(1)	N(9)–Co(2)–N(13)	84.2(1)
N(3)–Co(1)–N(3*)	180.0	N(11)–Co(2)–N(11*)	180.0
N(3)–Co(1)–N(5)	86.2(1)	N(11)–Co(2)–N(13)	85.9(2)
N(5)–Co(1)–N(5*)	180.0	N(13)–Co(2)–N(13*)	180.0
Co(1)–N(1)–N(2)	119.4(3)	Co(2)–N(9)–N(10)	120.7(3)
Co(1)–N(3)–N(4)	118.7(3)	Co(2)–N(11)–N(12)	117.6(3)
Co(1)–N(5)–N(6)	121.9(3)	Co(2)–N(13)–N(14)	119.2(3)

Table 5 Selected bond distances (Å) and bond angles (deg) for $[B(pz)_4]_2Ni$ (**4**)

	Molecule 1		Molecule 2
Ni(1)–N(1)	2.037(2)	N(2)–N(9)	2.070(2)
Ni(1)–N(3)	2.087(2)	N(2)–N(11)	2.088(2)
Ni(1)–N(5)	2.121(2)	N(2)–N(13)	2.087(2)
N(1)–Ni(1)–N(1*)	180.0	N(9)–Ni(2)–N(9*)	180.0
N(1)–Ni(1)–N(3)	87.62(8)	N(9)–Ni(2)–N(11)	86.73(9)
N(1)–Ni(1)–N(5)	86.55(8)	N(9)–Ni(2)–N(13)	87.21(8)
N(3)–Ni(1)–N(3*)	180.0	N(11)–Ni(2)–N(11*)	180.0
N(3)–Ni(1)–N(5)	85.05(8)	N(11)–Ni(2)–N(13)	85.60(8)
N(5)–Ni(1)–N(5*)	180.0	N(13)–Ni(2)–N(13*)	180.0
Ni(1)–N(1)–N(2)	118.3(1)	Ni(2)–N(9)–N(10)	117.6(2)
Ni(1)–N(3)–N(4)	121.0(1)	Ni(2)–N(11)–N(12)	119.4(2)
Ni(1)–N(5)–N(6)	118.8(1)	Ni(2)–N(13)–N(14)	120.9(2)

Table 6 Selected bond distances (Å) and bond angles (deg) for $[B(pz)_4]_2Cu$ (**5**)

	Molecule 1		Molecule 2
Cu(1)–N(1)	1.989(3)	Cu(2)–N(9)	2.017(3)
Cu(1)–N(3)	2.009(2)	Cu(2)–N(11)	2.023(3)
Cu(1)–N(5)	2.462(3)	Cu(2)–N(13)	2.382(3)
N(1)–Cu(1)–N(1*)	180.0	N(9)–Cu(2)–N(9*)	180.0
N(1)–Cu(1)–N(3)	87.6(1)	N(9)–Cu(2)–N(11)	86.9(1)
N(1)–Cu(1)–N(5)	83.5(1)	N(9)–Cu(2)–N(13)	82.4(1)
N(3)–Cu(1)–N(3*)	180.0	N(11)–Cu(2)–N(11*)	180.0
N(3)–Cu(1)–N(5)	85.0(1)	N(11)–Cu(2)–N(13)	86.6(1)
N(5)–Cu(1)–N(5*)	180.0	N(13)–Cu(2)–N(13*)	180.0
Cu(1)–N(1)–N(2)	119.0(2)	Cu(2)–N(9)–N(10)	118.7(2)
Cu(1)–N(3)–N(4)	123.4(2)	Cu(2)–N(11)–N(12)	122.3(2)
Cu(1)–N(5)–N(6)	111.0(2)	Cu(2)–N(13)–N(14)	113.9(2)

Table 7 Selected bond distances (Å) and bond angles (deg) for $[B(pz)_4]_2Zn$ (**6**)

	Molecule 1		Molecule 2
Zn(1)–N(1)	2.216(3)	Zn(2)–N(9)	2.128(4)
Zn(1)–N(3)	2.078(3)	Zn(2)–N(11)	2.159(3)
Zn(1)–N(5)	2.152(3)	Zn(2)–N(13)	2.151(3)
N(1)–Zn(1)–N(1*)	180.0	N(9)–Zn(2)–N(9*)	180.0
N(1)–Zn(1)–N(3)	85.2(1)	N(9)–Zn(2)–N(11)	85.4(1)
N(1)–Zn(1)–N(5)	83.6(1)	N(9)–Zn(2)–N(13)	86.3(1)
N(3)–Zn(1)–N(3*)	180.0	N(11)–Zn(2)–N(11*)	180.0
N(3)–Zn(1)–N(5)	86.5(1)	N(11)–Zn(2)–N(13)	84.3(1)
N(5)–Zn(1)–N(5*)	180.0	N(13)–Zn(2)–N(13*)	180.0
Zn(1)–N(1)–N(2)	117.8(2)	Zn(2)–N(9)–N(10)	116.9(3)
Zn(1)–N(3)–N(4)	118.1(2)	Zn(2)–N(11)–N(12)	118.6(3)
Zn(1)–N(5)–N(6)	121.0(2)	Zn(2)–N(13)–N(14)	121.0(3)

Table 8 Mean dimensions (Å or deg) of chelate rings in $[HB(pz)_3]_2Mn$ (**1**), $[B(pz)_4]_2Mn$ (**2**), $[HB(pz)_3]_2Fe$ (**7**), $[B(pz)_4]_2Fe$ (**8**), $[HB(pz)_3]_2Co$ (**9**), $[B(pz)_4]_2Co$ (**3**), $[HB(pz)_3]_2Ni$ (**10**), $[B(pz)_4]_2Ni$ (**4**), $[HB(pz)_3]_2Cu$ (**11**), $[B(pz)_4]_2Cu$ (**5**), $[HB(pz)_3]_2Zn$ (**12**), $[B(pz)_4]_2Zn$ (**6**), $[HB(pz)_3]_2Cd$ (**13**), $[B(pz)_4]_2Cd$ (**14**), $[HB(pz)_3]_2Mg$ (**15**), $[B(pz)_4]_2Mg$ (**16**), and $[HB(pz)_3]_2Ca$ (**17**)

	1	**7**[a]	**9**[b]	**10**[c]	**11**[d]	**12**[e]	**13**[f]	**15**[i]	**17**[i]
M–N1	2.25(3)	1.97(1)	2.13(1)	2.09(1)	2.17(21)	2.15(1)	2.33(3)	2.18(3)	2.44(2)
N1 ··· N1 (intraligand)	2.99(4)	2.75(1)	2.89(1)	2.87(1)	2.94(10)	2.93(1)	3.05(5)	2.94(4)	3.11(6)
N1 ··· N1 (interligand)	3.36(8)	2.83(1)	3.13(5)	3.04(3)	3.20(23)	3.16(5)	3.53(9)	3.23(7)	3.76(7)
M ··· B	3.29(1)	3.08(1)	3.20(1)	3.16(1)	3.21(1)	3.21(1)	3.35(1)	3.24(1)	3.46(1)
N1–M–N1	83.4(2.0)	88.3(0.2)	85.5(0.5)	86.8(0.4)	85.3(3.2)	85.6(0.3)	81.8(2.4)	84.7(2.0)	79.2(2.1)
M–N1–N2	117.8(1.2)	119.8(0.4)	119.1(0.3)	118.4(0.3)	117.6(4.1)	118.0(0.3)	117.6(1.1)	118.2(0.7)	118.2(0.6)
N1–N2–B	121.4(0.8)	117.9(0.4)	119.2(0.5)	119.7(0.2)	120.8(0.7)	120.4(0.3)	122.0(0.6)	120.7(0.6)	122.8(0.5)
N2–B–N2	109.4(0.8)	107.6(0.7)	108.9(0.7)	108.3(0.7)	108.9(1.3)	108.9(0.5)	110.0(1.1)	108.9(1.2)	110.4(0.6)

	2	**8**[g]	**3**	**4**	**5**	**6**	**14**[h]	**16**[i]
M–N1	2.24(3)	1.97(2)	2.12(3)	2.08(3)	2.15(20)	2.15(4)	2.33(4)	2.16(3)
N1 ··· N1 (intraligand)	2.95(4)	2.74(1)	2.88(2)	2.85(1)	2.92(11)	2.91(1)	3.02(6)	2.91(1)
N1 ··· N1(interligand)	3.36(8)	2.82(3)	3.12(5)	3.03(4)	3.17(19)	3.16(6)	3.54(11)	3.19(5)
M ··· B	3.31(1)	3.09(1)	3.20(1)	3.17(1)	3.19(1)	3.21(1)	3.38(1)	3.24(1)
N1–M–N1	82.7(2.3)	88.5(0.6)	85.3(1.1)	86.4(0.9)	85.3(1.9)	85.2(1.0)	80.8(2.8)	84.7(1.1)
M–N1–N2	119.2(1.9)	120.3(0.9)	119.6(1.4)	119.3(1.3)	118.1(4.4)	118.9(1.6)	118.5(2.0)	119.5(1.4)
N1–N2–B	119.8(2.4)	117.1(1.3)	119.0(2.0)	119.1(1.8)	119.5(2.0)	119.5(2.2)	120.9(2.5)	119.5(2.0)
N2–B–N2	109.0(0.9)	107.8(1.0)	108.6(1.3)	108.1(1.2)	108.8(1.2)	108.9(1.3)	109.1(0.8)	108.7(1.3)

top; $[HB(pz)_3]^-$, bottom; $[B(pz)_4]^-$.[a] Data taken from ref. 5*a*. [b] Data taken from ref. 5*b*. [c] Data taken from ref. 5*c*. [d] Data taken from ref. 5*d*. [e] Data taken from ref. 5*e*. [f] Data taken from ref. 5*f*. [g] Data taken from ref. 5*g*. [h] Data taken from ref. 5*h*. [i] Data taken from ref. 4*c*.

metal ions of six-coordination are 0.97 Å for Mn^{2+} (high-spin), 0.75 Å for Fe^{2+} (low-spin), 0.88 Å for Co^{2+} (high-spin), 0.83 Å for Ni^{2+}, 0.87 Å for Cu^{2+}, 0.88 Å for Zn^{2+} and 1.09 Å for Cd^{2+}; the M–N bond length is 2.29 Å for Mn–N, 2.07 Å for Fe–N, 2.21 Å for Co–N, 2.15 Å for Ni–N, 2.19 Å for Cu–N, 2.20 Å for Zn–N, and 2.46 Å for Cd–N. In the Cu(II) complexes, four Cu–N1 bonds are 2.0 Å and the remainder are 2.4 Å, so the coordination geometry of Cu(II) complexes is not C_3 symmetry but square bipyramid. The other complexes are C_3 symmetry and trigonally distorted octahedron. Deformation to widen the bite size (N1 ··· N1 distance) is necessary when $[HB(pz)_3]^-$ coordinates to a large ion such as Mn(II) and Cd(II). The deformation is the opening of the tripod of pyrazolyl rings and is realized chiefly by increasing the bond angles of N1–N2–B and N2–B–N2. However, there is a limitation in the deformation. Therefore, $[HB(pz)_3]^-$ coordinates to the large metal ions from further locations by widening the M ··· B distance and decreasing the bite angle (N1–M–N1). As a result, the trigonal distortion of donor atoms is enhanced [increase in the ratio of N1 ··· N1 (intraligand) to N1 ··· N1 (interligand)]. These features are similar to those observed for $[HB(pz)_3]_2Mg$ (**15**) and $[HB(pz)_3]_2Ca$ (**17**).[4c]

Table 9 Absolute values of dihedral angles (deg) for $[HB(pz)_3]_2Mn$ (**1**), $[B(pz)_4]_2Mn$ (**2**), $[HB(pz)_3]_2Fe$ (**7**), $[B(pz)_4]_2Fe$ (**8**), $[HB(pz)_3]_2Co$ (**9**), $[B(pz)_4]_2Co$ (**3**), $[HB(pz)_3]_2Ni$ (**10**), $[B(pz)_4]_2Ni$ (**4**), $[HB(pz)_3]_2Cu$ (**11**), $[B(pz)_4]_2Cu$ (**5**), $[HB(pz)_3]_2Zn$ (**12**), $[B(pz)_4]_2Zn$ (**6**), $[HB(pz)_3]_2Cd$ (**13**), and $[B(pz)_4]_2Cd$ (**14**)

	1	**7**[a]	**9**[b]	**10**[c]	**11**[d]	**12**[e]	**13**[f]
M–N1–N2–B	3.6(1.6)	1.8(1.6)	1.5(1.0)	1.4(0.6)	3.6(2.9)	1.2(0.7)	4.6(2.6)
M–N1–N2–C3	178.4(1.3)	178.3(1.4)	175.5(2.5)	175.7(2.8)	176.8(2.1)	175.8(2.4)	179.1(1.1)
	2	**8**[g]	**3**	**4**	**5**	**6**	**14**[h]
M–N1–N2–B	11.2(6.1)	2.3(1.2)	4.4(2.7)	4.0(2.8)	10.1(6.4)	5.0(3.4)	14.7(7.8)
M–N1–N2–C3	167.6(8.0)	173.8(3.6)	170.6(6.3)	171.1(5.9)	166.9(13.7)	170.0(7.3)	163.5(9.4)

top; $[HB(pz)_3]^-$, bottom; $[B(pz)_4]^-$. [a] Data taken from ref. 5*a*. [b] Data taken from ref. 5*b*. [c] Data taken from ref. 5*c*. [d] Data taken from ref. 5*d*. [e] Data taken from ref. 5*e*. [f] Data taken from ref. 5*f*. [g] Data taken from ref. 5*g*. [h] Data taken from ref. 5*h*.

Intraligand contact by a noncoordinated pyrazolyl ring in $[B(pz)_4]^-$

Table 8 shows that the bond lengths and angles of $[B(pz)_4]^-$ complexes are nearly equal to those of $[HB(pz)_3]^-$ complexes. However, the standard deviations in bond lengths and angles of the former are larger than those of the latter. Fig. 5 (right)

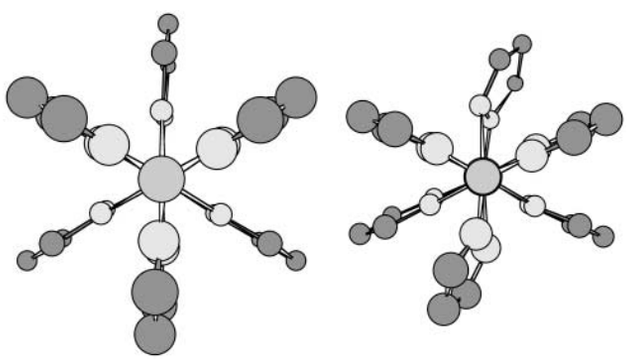

Fig. 5 (left) A ball and stick model of $[HB(pz)_3]_2Fe$ (**7**). (right) A ball and stick model of $[B(pz)_4]_2Cu$ (**5**). Both models are viewed from the B ··· M ··· B axis. The fourth pyrazolyl ring of **5** is not shown for clarity.

shows a ball and stick model of $[B(pz)_4]_2Cu$ (**5**) viewed from the B ··· M ··· B axis. The fourth pyrazolyl ring is not shown for clarity. It is obvious that two coordinated pyrazolyl groups, one from each ligand and oriented *trans*, are tilted. The tilt is reflected by dihedral angles, such as M–N1–N2–B and M–N1–N2–C3 (Table 9). These dihedral angles should be 0° and 180°, respectively, when the C_3 symmetry is perfect. The results in Table 9 suggest that the symmetry of $[B(pz)_4]^-$ complexes is decreased. This should be attributed to intraligand contact caused by the fourth bulky pyrazolyl ring on the boron atom of $[B(pz)_4]^-$. When the free ligand is taken from the lowest strain energy configuration and coordinated to a metal ion in a tripodal tridentate fashion with a bite size of 2.9 Å, the increase in strain energy is 5.2 kcal mol^{-1}.[4d] The steric energy sharply increases with the increase in bite size. The increased strain energy in complex formation should decrease the stability constant. When $[B(pz)_4]^-$ widens the bite size so as to coordinate large metal ions, such as Mn(II) and Cd(II), the steric repulsion between the coordinated and noncoordinated pyrazolyl rings is enhanced. The M–N1–N2–B and M–N1–N2–C3 angles suggest that two pyrazolyl groups are substantially tilted for $[B(pz)_4]_2Mn$ (**2**) and $[B(pz)_4]_2Cd$ (**14**) complexes. It is most likely that the strain energy accompanying complexation becomes large and the stability constant is decreased more for these large metal ions. Consequently, $[B(pz)_4]^-$ extracts Mn(II) and Cd(II) at higher pH than $[HB(pz)_3]^-$.

The unusual features of Cu(II) complexes

As shown in Table 1, the log K_{ex} for $[HB(pz)_3]^-$ increases in the order of Mn(II), Fe(II), Co(II), Ni(II) and Cu(II), and decreases in the order of Zn(II) and Cd(II). This tendency obeys the Irving–Williams series. In contrast, the tendency of $[B(pz)_4]^-$ is distinct. The log K_{ex} of Ni(II) is higher than the other metals. The log K_{ex} of Cu(II) for $[B(pz)_4]^-$ is smaller than that for $[HB(pz)_3]^-$. The data obtained by X-ray diffraction are also used to focus on the differences between Cu(II) complexes and other complexes. Because of the Jahn–Teller effect, the Cu(II) complexes are tetragonally distorted. In order to increase the M–N1 distance, the *z*-axis pyrazolyl group is tilted backward. The tilting is obvious in the angle M ··· B ··· C3. Although this angle is 90.4–93.3 for Co(II) and Zn(II) complexes, it is 95.8–102.6 for the *z*-axis pyrazolyl group in $[HB(pz)_3]_2Cu$ (**11**) and $[B(pz)_4]_2Cu$ (**5**). The dihedral angles of M–N1–N2–B and M–N1–N2–C3 for **11** are nearly equal to those of $[HB(pz)_3]_2Co$ (**9**) and $[HB(pz)_3]_2Zn$ (**12**) (Table 9). In contrast, the dihedral angles for **5** are different from those of $[B(pz)_4]_2Co$ (**3**) and $[B(pz)_4]_2Zn$ (**6**). For **5**, the tilt for the *z*-axis pyrazolyl group is substantially enhanced. These results suggest that the formation of **5** is accompanying a larger strain energy increase than **3** and **6** because of the intraligand contact between the pyrazolyl rings from the *z*-axis and noncoordinated pyrazolyl rings. Although **11** can realize the tetragonal distortion without the tilt of the *z*-axis pyrazolyl group, **5** must tilt the *z*-axis pyrazolyl group due to intraligand contact. This intraligand contact decreases the K_{ex} of **5** compared with that of **11**.

Experimental

General procedures

$K[HB(pz)_3]$ and $K[B(pz)_4]$ were synthesized as previously reported.[8] All other chemicals were reagent-grade and distilled water was used throughout. Proton NMR spectra were obtained at 25 ± 1 °C using a JEOL LA 400 spectrometer. Chemical shifts are reported (ppm) downfield from TMS as an internal standard. The reported ^1H coupling constants are $^3J_{HH}$ values.

Distribution of poly(pyrazolyl)borates

Acid dissociation and partition constants of poly(pyrazolyl)-borates were studied by liquid–liquid extraction. An aliquot of chloroform (10 mL) was equilibrated with an equal volume of an aqueous phase containing 5×10^{-3} M of $K[HB(pz)_3]$ or $K[B(pz)_4]$ buffered with 1×10^{-2} M of sodium acetate, 2-(*N*-morpholino)ethanesulfonic acid (MES), 3-(*N*-morpholino)-propanesulfonic acid (MOPS), *N*-tris(hydroxymethyl)methyl-3-aminopropanesulfonic acid (TAPS), 2-(cyclohexylamino)-ethanesulfonic acid (CHES) or 3-cyclohexylaminopropane-sulfonic acid (CAPS) at 25 ± 1 °C. After the two phases were

Table 10 Selected crystallographic data for $[HB(pz)_3]_2Mn$ (**1**), $[B(pz)_4]_2Mn$ (**2**), $[B(pz)_4]_2Co$ (**3**), $[B(pz)_4]_2Ni$ (**4**), $[B(pz)_4]_2Cu$ (**5**), and $[B(pz)_4]_2Zn$ (**6**)

	1	**2**	**3**	**4**	**5**	**6**
Empirical formula	$C_{18}H_{20}N_{12}B_2Mn$	$C_{24}H_{24}N_{16}B_2Mn$	$C_{24}H_{24}N_{16}B_2Co$	$C_{24}H_{24}N_{16}B_2Ni$	$C_{24}H_{24}N_{16}B_2Cu$	$C_{24}H_{24}N_{16}B_2Zn$
Formula weight	480.99	613.12	617.11	616.88	621.73	623.56
Crystal size/mm	0.4 × 0.2 × 0.6	0.5 × 0.3 × 0.2	0.3 × 0.2 × 0.5	0.4 × 0.2 × 0.5	0.3 × 0.15 × 0.6	0.2 × 0.1 × 0.4
Crystal system	Monoclinic	Monoclinic	Triclinic	Triclinic	Triclinic	Triclinic
Space group (no.)	*C*2/*c* (No. 15)	$P2_1/c$ (No. 14)	$P\bar{1}$ (No. 2)	$P\bar{1}$ (No. 2)	$P\bar{1}$ (No. 2)	$P\bar{1}$ (No. 2)
a/Å	18.968(2)	7.741(2)	12.090(2)	12.041(2)	12.030(1)	12.1261(9)
b/Å	13.709(2)	9.872(2)	12.279(2)	12.285(2)	12.516(2)	12.2786(9)
c/Å	19.045(2)	17.991(1)	9.773(1)	9.723(1)	9.567(1)	9.8093(7)
α/deg			95.42(1)	95.60(1)	90.19(1)	95.250(6)
β/deg	111.352(8)	92.094(10)	102.85(1)	102.47(1)	101.749(9)	103.163(6)
γ/deg			100.00(1)	99.91(1)	78.812(10)	100.019(6)
V/Å^3	4612(1)	1373.9(4)	1379.6(4)	1369.7(4)	1382.5(3)	1387.3(2)
Z	8	2	2	2	2	2
$d_{calc.}$/g cm^{-3}	1.385	1.482	1.485	1.496	1.493	1.493
μ/cm^{-1}	49.29	43.17	52.82	14.28	15.18	16.31
2*θ* range/deg	5–140	5–140	5–120	5–120	5–120	5–120
Collected reflections	4250	2914	4332	4304	3923	4351
Unique reflections	4134	2704	4106	4079	3727	4125
Observed reflections	2641	1963	3333	3580	3103	3165
Refined parameters	300	197	392	392	392	392
R	6.4	4.7	5.4	3.6	4.0	4.4
R_w	7.9	5.9	6.8	5.6	5.6	5.4
Goodness of fit	1.66	1.27	1.73	1.68	1.59	1.57

separated by centrifugation, the pH of the aqueous phase was measured. The ligand concentration in the aqueous phase was determined from the boron content using a Japan Jarrell Ash ICAP-500 inductively coupled argon plasma emission spectrometer. The concentration in the organic phase was measured after back-extraction into 10^{-2} M sodium hydroxide.

Extraction of first-series transition metal and cadmium(II) ions

An aliquot of chloroform (10 mL) was shaken with an equal volume of an aqueous phase containing 1×10^{-2} M of $K[HB(pz)_3]$ or $K[B(pz)_4]$ and a metal ion (1×10^{-4} M) at 25 ± 1 °C. The pH of the aqueous phase was adjusted with hydrochloric acid or acetic acid (1×10^{-1} M) to study the effect of shaking time and pH on the percentage extraction (%*E*). The metal concentration in the aqueous phase was determined using a HITACHI Z-8100 polarized Zeeman spectrophotometer or ICAP-500. The concentration in the organic phase was measured after back-extraction into 4 M hydrochloric acid. The extraction constant (K_{ex}) was determined in the aqueous phase where the sum of the concentrations of hydrochloric acid and lithium chloride was 1.5 M, and the concentration was 10^{-3} M for the ligands and 10^{-5} M for the metal ions.

Preparation of the complexes

$[HB(pz)_3]_2Mn$ (**1**), $[B(pz)_4]_2Mn$ (**2**), $[B(pz)_4]_2Co$ (**3**), $[B(pz)_4]_2$-Ni (**4**), $[B(pz)_4]_2Cu$ (**5**), and $[B(pz)_4]_2Zn$ (**6**) were prepared using similar procedures. The preparation of $[HB(pz)_3]_2Mn$ (**1**) is shown below and the remaining procedures are given in the ESI.† The preparation of these complexes was described previously by Trofimenko,[8a] although he prepared them by mixing only the appropriate metal ion and $K[HB(pz)_3]$ or $K[B(pz)_4]$, so the purification procedure was complicated.

Bis[hydrotris(pyrazolyl)borato]manganese(II), $[HB(pz)_3]_2Mn$ (1)

Eighty milliliters of 0.05 M sodium hydroxide containing $K[HB(pz)_3]$ (1.513 g, 6.0 mmol) was added to 1 M hydrochloric acid (10 mL) containing $MnCl_2 \cdot 4H_2O$ (0.594 g, 3.0 mmol). Sodium hydroxide (1 M) was added and mixed until a white precipitate no longer formed (pH 2.5). After 20 min, the precipitate was filtered off and washed with distilled water and methanol. Crystals for the analytical sample and the X-ray structure were obtained by recrystallization from a mixture of dichloromethane and acetonitrile in a 1 : 2 volume ratio. Anal. Calcd for $C_{18}H_{20}N_{12}B_2Mn$: C, 44.95; H, 4.19; N, 34.94. Found: C, 45.00; H, 4.10; N, 35.13%.

X-Ray structure determination

Crystallographic data are summarized in Table 10. Crystals of **1**–**6** were mounted onto fine glass fibers with epoxy cement. The lattice parameters and intensity data were measured on a Rigaku AFC7R four-circle diffractometer with Ni-filtered Cu-Kα radiation (λ = 1.54178 Å) at 20 ± 1 °C. An ω–2θ scan to maximum 2θ values of 120–140° was used. An empirical absorption correction using the program DIFABS[9] was applied to **4**, and that based on azimuthal scans of several reflections was applied to the other complexes. The data were corrected for Lorentz and polarization effects. A correction for secondary extinction was applied. The structures were solved by direct methods[10] and expanded using Fourier techniques.[11] The non-hydrogen atoms were refined anisotropically. Hydrogens were fixed at the positions generated by calculation. All calculations were performed using the teXsan crystallographic software package developed by the Molecular Structure Corporation.

CCDC reference numbers 172046–172051.

See http://www.rsc.org/suppdata/dt/b1/b106006f/ for crystallographic data in CIF or other electronic format.

References

1 (*a*) R. D. Hancock and A. E. Martell, *Chem. Rev.*, 1989, **89**, 1875; (*b*) R. D. Hancock, *Prog. Inorg. Chem.*, 1989, **37**, 187; (*c*) A. E. Martell and R. D. Hancock, *Metal Complexes in Aqueous Solutions*, Plenum Press, New York, 1996.

2 S. Umetani, Y. Kawase, H. Takahara, L. T. H. Quyen and M. Matsui, *J. Chem. Soc., Chem. Commun.*, 1993, 78.

3 R. M. Izatt, K. Pawlak, J. S. Bradshaw and R. L. Bruening, *Chem. Rev.*, 1991, **91**, 1721.

4 (*a*) Y. Sohrin, H. Kokusen, S. Kihara, M. Matsui, Y. Kushi and M. Shiro, *Chem. Lett.*, 1992, 1461; (*b*) N. Yasuda, H. Kokusen, Y. Sohrin, S. Kihara and M. Matsui, *Bull. Chem. Soc. Jpn.*, 1992, **65**, 781; (*c*) Y. Sohrin, H. Kokusen, S. Kihara, M. Matsui, Y. Kushi and M. Shiro, *J. Am. Chem. Soc.*, 1993, **115**, 4128; (*d*) Y. Sohrin, M. Matsui, Y. Hata, H. Hasegawa and H. Kokusen, *Inorg. Chem.*, 1994, **33**, 4376; (*e*) H. Kokusen, Y. Sohrin, H. Hasegawa, S. Kihara and M. Matsui, *Bull. Chem. Soc. Jpn.*, 1995, **68**, 172; (*f*) H. Kokusen, Y. Sohrin, M. Matsui, Y. Hata and H. Hasegawa, *J. Chem. Soc., Dalton Trans.*, 1995, 195.

5 (*a*) J. D. Oliver, D. F. Mullica, B. B. Hutchinson and W. O. Milligan, *Inorg. Chem.*, 1980, **19**, 165; (*b*) M. R. Churchill, K. Gold and C. E. Maw, Jr., *Inorg. Chem.*, 1970, **9**, 1597; (*c*) G. Bandoli, D. A. Clemente, G. Paolucci and L. Doretti, *Cryst. Struct. Commun.*, 1979, **8**, 965; (*d*) A. Murphy, B. J. Hathaway and T. J. King, *J. Chem. Soc., Dalton Trans.*, 1978, 1646; (*e*) K. Nakata, S. Kawabata and K. Ichikawa, *Acta Crystallogr., Sect. C*, 1995, **51**, 1092; (*f*) D. L. Reger, S. M. Myers, S. S. Mason, D. J. Darensbourg, M. W. Holtcamp, J. H. Reibenspies, A. S. Lipton and P. D. Ellis, *J. Am. Chem. Soc.*, 1995, **117**, 10998; (*g*) Y. Sohrin, H. Kokusen and M. Matsui, *Inorg. Chem.*, 1995, **34**, 3928; (*h*) D. L. Reger, S. S. Mason, A. L. Rheingold and R. L. Ostrander, *Inorg. Chem.*, 1993, **32**, 5216.

6 D. D. Perrin, *Stability Constants of Metal-Ion Complexes, Part B, Organic Ligands*, IUPAC Chemical Data Series 22, Pergamon Press, Oxford, 1979, p. 103.

7 R. D. Shannon, *Acta Crystallogr., Sect. A*, 1976, **32**, 751 . The radius of the nitrogen atom is taken as 1.32 Å of four-coordinate N^{3-}.

8 (*a*) S. Trofimenko, *J. Am. Chem. Soc.*, 1967, **89**, 3170; (*b*) S. Trofimenko, *Scorpionates—The Coordination Chemistry of Poly(pyrazolyl)borate Ligands*, Imperial College Press, London, 1999.

9 N. Walker and D. Stuart, *Acta Crystallogr., Sect. A*, 1983, **39**, 158.

10 (*a*) G. M. Sheldrick, in *Crystallographic Computing*, ed. G. M. Sheldrick, C. Kruger and R. Goddard, Oxford University Press, Oxford, England, 1985, vol. 3, pp. 175; (*b*) M. C. Burla, M. Camalli, G. Cascarano, C. Giacovazzo, G. Polidori, R. Spagna and D. Viterbo, *J. Appl. Crystallogr.*, 1989, **22**, 389; (*c*) A. Altomare, M. C. Burla, M. Camalli, M. Cascarano, C. Giacovazzo, A. Guagliardi and G. Polidori, *J. Appl. Crystallogr.*, 1994, **27**, 435.

11 P. T. Beurskens, G. Admiraal, G. Beurskens, W. P. Bosman, R. de Gelder, R. Israel and J. M. M. Smits, The DIRDIF-94 program system, Technical Report of the Crystallography Laboratory, University of Nijmengen, The Netherlands, 1994.